

Semi-automatic Data Annotation System for Multi-Target Multi-Camera Vehicle Tracking

Haohong Liao^{1,2}, Silin Zheng^{1,2}, Xuelin Shen², Mark Junjie Li¹, Xu Wang^{1*}

¹ College of Computer Science and Software Engineering, Shenzhen University, Shenzhen, China

² Guangdong Laboratory of Artificial Intelligence and Digital Economy, ShenZhen, China

liaohaohong2021@email.szu.edu.cn, zhengpny@gmail.com, shenxuelin@gml.ac.cn, {jj.li, wangxu}@szu.edu.cn

Abstract—Multi-target multi-camera tracking (MTMCT) plays an important role in intelligent video analysis, surveillance video retrieval, and other application scenarios. Nowadays, the deep-learning-based MTMCT has been the mainstream and has achieved fascinating improvements regarding tracking accuracy and efficiency. However, according to our investigation, the lacking of datasets focusing on real-world application scenarios limits the further improvements for current learning-based MTMCT models. Specifically, the learning-based MTMCT models training by common datasets usually cannot achieve satisfactory results in real-world application scenarios. Motivated by this, this paper presents a semi-automatic data annotation system to facilitate the real-world MTMCT dataset establishment. The proposed system first employs a deep-learning-based single-camera trajectory generation method to automatically extract trajectories from surveillance videos. Subsequently, the system provides a recommendation list in the following manual cross-camera trajectory matching process. The recommendation list is generated based on side information, including camera location, timestamp relation, and background scene. In the experimental stage, extensive results further demonstrate the efficiency of the proposed system.

Index Terms—Multi-Object Tracking, Multi-Target Multi-Camera Tracking, Vehicle Re-Identification, Semi-Automatic, Data Annotation.

I. INTRODUCTION

Multi-target multi-camera tracking (MTMCT) is an important technology in intelligent transportation, city brain, intelligent video analysis, *etc.* It aims to model vehicles' trajectories from multi-camera surveillance videos, contributing to vehicle tracking and traffic flow analysis and prediction. The core of MTMCT is to compare the target vehicle from a certain camera view to a gallery of candidates captured by nearby cameras. In the past decade, the rapid development of machine learning technology shed new light on MTMCT studies. And the learning-based MTMCT has been the mainstream nowadays. The learning-based MTMCT methods [1]–[5] share a similar pipeline: the object detection and vehicle re-identification (re-ID) technologies are employed to detect the target vehicle and extract the corresponding features, respectively. Then, the extracted features and the bounding boxes would be fed into multi-object tracking (MOT) module for trajectory generation, sequence-level clustering and cross-camera trajectory feature representation.

For the learning-based methods, the fundamental and indispensable work is establishing a steady and convincing

dataset containing a wide variety of content and a sufficient number of trajectory annotations. Unlike the datasets of common computer vision tasks, the MTMCT datasets do not only require labeling the targets within the video but also matching targets across videos from different cameras. Conventional MTMCT datasets, such as CAVIAR4ReID [6], WARD [7] are constructed via manually labeling, which limits the dataset scale. Learning-based MTMCT models trained by these datasets usually cannot achieve satisfactory results. Recently, some works have leveraged cutting-edge deep-learning technologies (such as ACF [8] and Faster R-CNN [9]) to realize automatic annotation. Compared with the manually labeled datasets, which are usually at the thousand-level scales, the semi-automatic annotation method allows for establishing million-level scale datasets, such as MARS [10], MSMT17 [11], *etc.*

Although favorable achievements have been made in recent years, recent works [12] [13] have revealed the limitations caused by existing datasets. Specifically, the learning-based MTMCT models trained by common datasets cannot achieve satisfactory results in real-world application scenarios due to the domain gap. Under this circumstance, a feasible way is especially establishing a dataset according to the actual application scenario. To this end, we propose a semi-automatic MTMCT data annotation system. To the best of our knowledge, it is the first semi-automatic annotation system focusing on the MTMCT dataset. The architecture of proposed system is shown in Fig. 1. The main contributions can be summarized as follows:

- A deep-learning-based single-camera trajectory generation method is proposed in our system, where cutting-edge object detection and MOT models are employed to generate the vehicle trajectories automatically. After the automatic trajectory generation, the users will be asked to match the cross-camera vehicle trajectories. At this stage, the proposed system provides recommendation lists by making full use of side information (including camera location, timestamp, and background scene), significantly improving the manual labeling accuracy and efficiency.
- Regarding the system optimization, we propose a novel visualization strategy that dynamically generates the labeled videos via stored trajectory features. It saves plenty of storage requirements compared with the conventional

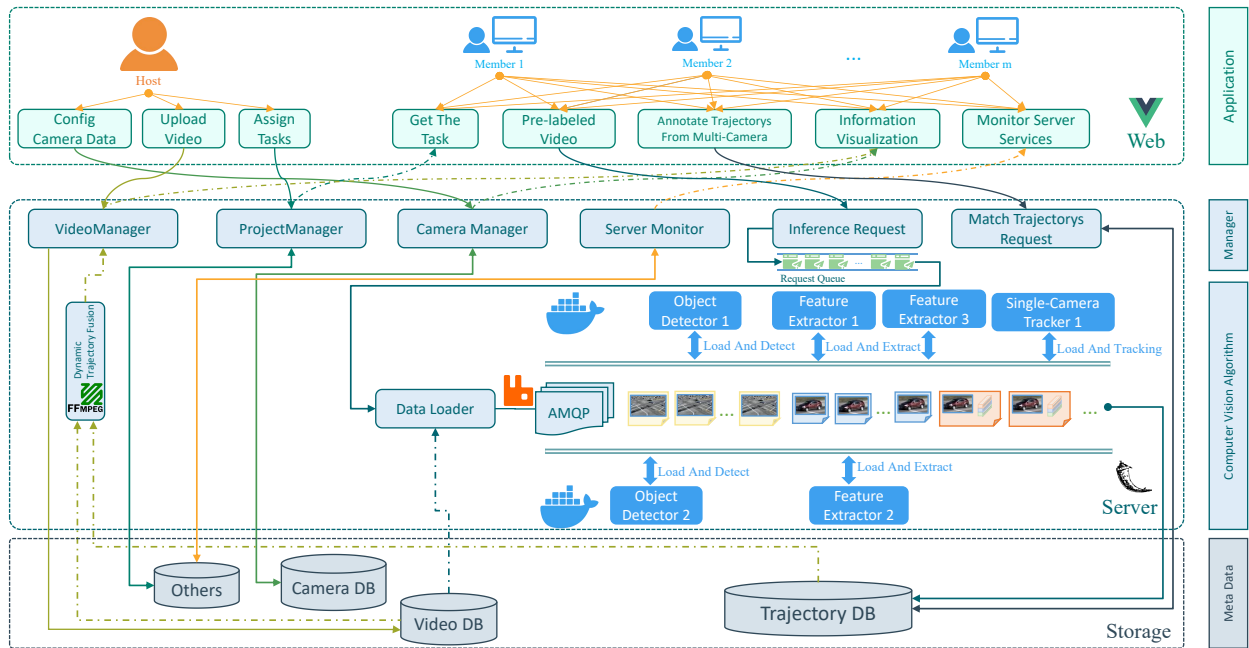


Fig. 1. The architecture of proposed system.

method of directly saving the annotated video. Moreover, we employ the Linux Container technology and advanced message queuing protocol (AMQP) to improve the system's scalability.

- In the experimental stage, we validate the proposed system's efficiency based on the CityFlow [14] dataset. Experimental results have demonstrated the accuracy of proposed deep-learning-based single-camera trajectory generation method, the efficiency of employed optimization strategy.

II. RELATED WORK

A. MTMCT

The paradigm of MTMCT is illustrated in Fig. 2. There are several sub-tasks within the MTMCT pipeline: (1) MOT, aims at extracting the trajectory feature vectors of the target vehicle from single-camera surveillance video. (2) Vehicle re-ID, retrieves the target vehicle in a massive gallery set. (3) Trajectory clustering, employs the spatial-temporal relation of related cameras to cluster target vehicle's cross-camera trajectory features. In recent years, deep-learning-based MTMCT models have been rapidly developed. However, there are still many challenges. In actual application scenarios, the occlusion, complex lighting conditions, and low video resolutions cause great trouble for MTMCT models. Focusing on this, Liu *et al.* [2] employs TFS filtering and DBTM constraint matching successfully increase the recall rate. Ye *et al.* [3] employ the TPM algorithm to overcome the influence caused by occlusion.

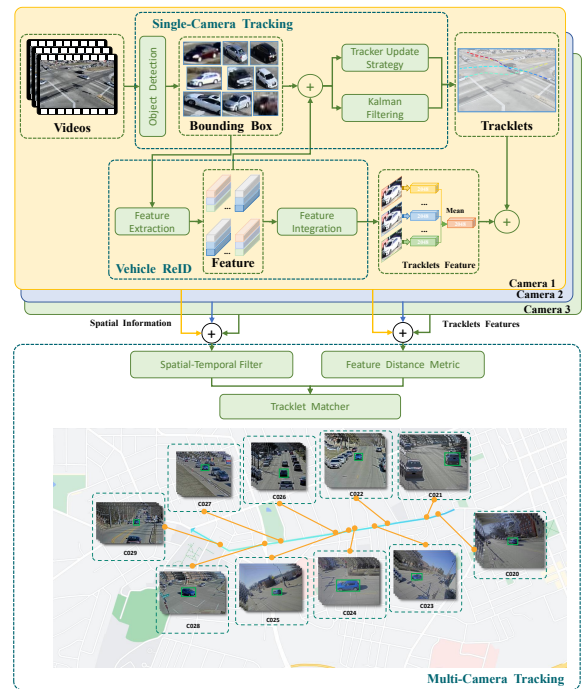


Fig. 2. Illustration of Multi-Target Multi-Camera Tracking pipeline.

B. Existing Dataset

As exhibited in table I, we summarize the existing person and vehicle re-ID datasets from the aspects of dataset scale, target number, and camera diversity. As shown, most of the existing datasets are based on manual labeling, which is extremely time-consuming [14], [25]–[28]. As for VRAI [27],

TABLE I
SUMMARY OF REID DATASET.

Type	Dataset	Release Time	Cams	Imgs	IDs	Video	Multiview	Geom.	Label Method
PersonReID	VIReR [15]	2007	2	1,264	632	×	×	×	Hand
	GRID [16]	2009	8	1,275	1,025	×	×	×	Hand
	3DPes [17]	2011	8	192	1,011	×	✓	×	Hand
	PRID2011 [18]	2011	2	1,134	200	✓	✓	×	Hand
	CUHK01 [19]	2012	2	3,884	971	×	✓	×	Hand
	CUHK02 [20]	2013	10	7,264	1,816	×	✓	×	Hand
	CUHK03 [21]	2014	10	13,164	1,467	×	×	×	DPM [22]/Hand
	Market-1501 [23]	2015	6	32,668	1,501	×	✓	×	DPM [22]/Hand
	MARS [10]	2016	6	20,715	1,261	×	✓	×	DPM [22]+GMMCP [1]
	DukeMTMC-reID [24]	2017	8	36,411	1,404	×	✓	×	Hand
MSMT17 [11]	2018	15	126,441	4,101	×	✓	×	Faster R-CNN [9]	
VehicleReID	VIRi-776 [25]	2016	20	49,357	776	×	✓	✓	Hand
	VehicleID [26]	2016	2	221,763	26,267	×	✓	×	Hand
	VRAI [27]	2019	2	137,613	13,022	×	✓	×	Hand
	CityFlow [14]	2019	40	229,680	666	✓	✓	✓	Object Detection+MOT
	VeRi-Wild [28]	2019	174	416,314	40,671	×	✓	✓	YOLOv2 [29]

it spends around 1,000 hours to label the single vehicle bounding boxes, and 2,500 hours for cross-camera vehicle matching. Finally, 13,022 vehicle identifications are generated. Recently, thanks to the rapid development of machine learning technology, deep-learning-based pre-labeling [10], [11], [14], [21], [23], [28] are proposed to save the resource requirement. Take VeRi Wild [28] as example, the vehicle bounding boxes are labeled via Yolov2 [29], and 11 volunteers are invited to clean and organize 12 million original images for a month, finally collecting 40,671 vehicle identifications and 416,314 images.

Besides the datasets based on images, in order to handle application scenarios requiring temporal domain information, datasets focusing on videos have been proposed, such as MARS [10], and CityFlow [14]. However, the constructions of video-based datasets are extremely time-consuming since they require manual labeling frame by frame. Under this circumstance, many deep-learning-based automatic labeling methods have been proposed [13], [30]–[33]. As for [30] [31], they employed reinforcement learning to achieve faster data iteration and train a re-ID network with manual loop supervision strategy. In [32] [33], the authors employed generative adversarial network (GAN) models to generate virtual image domain datasets focusing on digital city and digital twin. The dataset construction process barely requires manual labeling. In [13], Zhao *et.al.* proposed a semi-automatic labeling method for re-ID dataset. However, this method still requires plenty of manual data cleaning and sorting.

III. THE PROPOSED SEMI-AUTOMATIC DATA ANNOTATION SYSTEM

This section details the proposed semi-automatic MTMCT data annotation system. We first describe the deep-learning-based single-camera trajectory extraction. Then, the provided manual matching assistance is detailed. At last, we present the efforts for system optimization regarding data visualization and adaptability.

A. Deep-Learning-Based Single-Camera Trajectory Generation

Single-camera trajectory generation plays an important role in the proposed system, whose performance is directly related to the accuracy of the multi-camera matching. Single-camera trajectory extraction mainly comprises two subtasks: MOT and trajectory feature generation. As for a set of raw video sequences from different cameras, the proposed system will first sample key frames with a constant interval. The YOLOv5 [29] algorithm is subsequently employed to detect all vehicles in each frame and return their bounding boxes. Then, features of detected vehicles will be extracted via a well-trained re-ID model. Finally, the extracted features will be fed into the DeepSort [34] algorithm for single-camera trajectory generation. As for the other frames, their trajectories would be inferred by a linear interpolation method, which would save great storage and computation resources. Specifically, denote the frame sample interval as f , and the bounding box of the frame i as $b_i = (x_1^i, y_1^i, x_2^i, y_2^i)$. Then the bounding boxes of frame $j \in [I, i + f]$ can be inferred by the Eq. (1),

$$b_j = b_i + \frac{j-i}{f} \times (b_{i+f} - b_i), \quad (1)$$

Finally, following the method proposed in [2], the single-shot trajectory features from selected sequence is generated by,

$$T = \frac{1}{N} \sum_{i=0}^N f_i, \quad (2)$$

where N denotes the total frame number, and f_i the feature vector of i -th. frame. In the process of end-to-end trajectory extraction, we reduce the confidence threshold of the object detector to improve the recall rate of vehicle trajectories, but it will lead to a large number of false-positive samples. Therefore, we eliminate a large number of static targets and false detection samples according to the duration and the moving distances of the extracted trajectories.

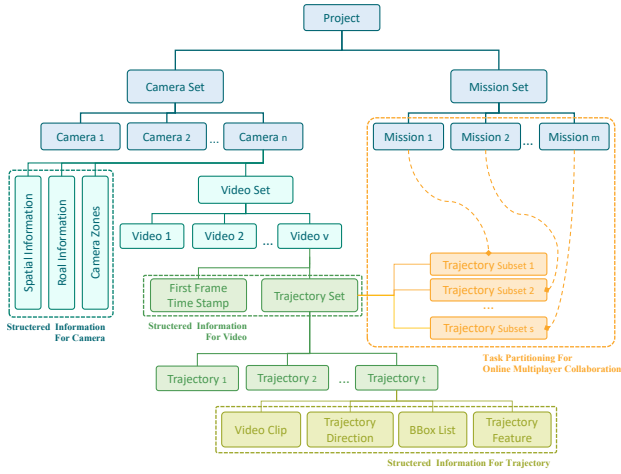


Fig. 3. Employed side information for cross-camera trajectory matching in the proposed system.

B. Manual Cross-Camera Trajectory Matching Assistance

After the single-camera trajectory extraction, users will match trajectories from different cameras to construct the MTMCT dataset. In this stage, the system provides a list of trajectories from nearby cameras for the target vehicle. In this process, the target occlusion, pose variance caused by shooting angle, lighting condition variance, and poor video quality make it hard for the system to generate reliable recommendation lists. Additionally, the similarities among the vehicles' shapes and colors usually cause great trouble for users' matching process. Under these circumstances, the system makes full use of side information to establish reliable recommendation lists, and provide extra assistance for manual matching. Fig. 3 shows the employed side information. This subsection details the generation of the side information.

1) **Recommendation List Construction Based On Times-tamp:** As for the target vehicle, the system would first provide a recommendation list for cross-camera matching. The candidates are usually selected according to their appearance time-window in corresponding cameras' surveillance videos. However, previous methods failed to consider the situation in actual application scenarios, where there are usually overlapping shoot areas among nearby surveillance cameras. This usually causes incomplete recommendation lists, compromising the matching accuracy. To this end, we employ Algorithm 1 to get the maximum range of possible entry-time of the target under the downstream camera, and Algorithm 2 to construct sorted gallery (CSG). Take the two adjacent surveillance cameras A and B with overlapping shooting areas as an example, where A is in front of B . The basic idea is that, the target's entry time-point of B is allowed being before or after the entry time-point of A , but must before the exit time-point of A .

2) **Recommendation List Cleaning based on Camera Location:** The cameras' location information will also be structured and employed to help construct the candidate list. The basic idea is that, one vehicle's appearance time-point at corresponding cameras should be related to the cameras'

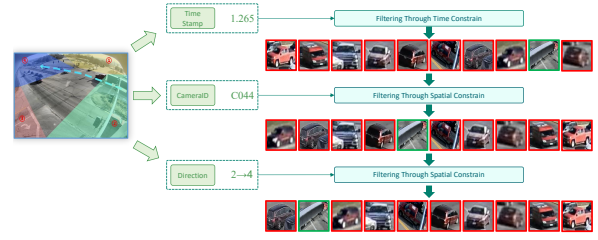


Fig. 4. Illustration of recommendation list construction based on employed side information.

Algorithm 1 Construct Gallery Filter By Time Constrain

Require: C (dict of camera), O (overlap time with query camera), st (start time of trajectory), et (end time of trajectory)
Input: C_1 (list of gallery cameras), Q (trajectory in query set)
Output: G (list of gallery after time constraint)

- 1: **for** $c \in C_1$ **do**
- 2: **if** area of c overlap with C_2 **then**
- 3: $st_{sch} \leftarrow st_Q - O$
- 4: **else**
- 5: $st_{sch} \leftarrow st_Q$
- 6: $g \leftarrow CSG(st_{sch}, G_c, Min, Max)$
- 7: $G \leftarrow G \cup g$
- 8: **return** G

locations [2]. Specifically, the target vehicle's single-camera-trajectory cannot be matched to trajectories from cameras that are too far away. Besides, the basic traffic rules are also contributed to constructing the recommendation list. Take the Fig. 4 as an example, if the vehicle drives from the No.2 area to the No.4 area, trajectory candidates from cameras in No.1 and No.3 would be discarded. Moreover, as shown in Fig. 5, the structured camera location information is not only contributed to the candidate list construction but also be visualized and provided to users, which would be helpful in manual trajectory matching.

3) **Side Information for Manual Matching Assistant:** The system also provides the original video clips of candidates to users, which greatly improves the matching accuracy in complex situations (such as indistinguishable vehicle shapes, occlusions, etc.). An example is shown in Fig. 6, users can easily distinguish similar vehicles according to the contained background scene with the provided video clips, avoiding

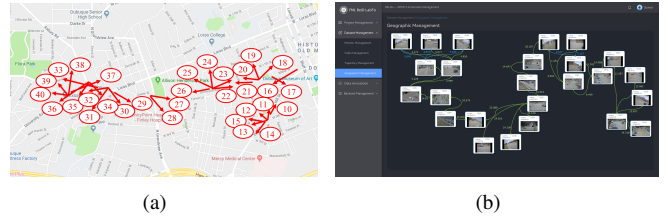


Fig. 5. Illustration of camera location information. (a) Camera location map in CityFlow; (b) Extracted camera location information.

Algorithm 2 $CSG(st_{sch}, G_c, Min, Max)$

Require: j (dict of single camera trajectory)**Input:** st_{sch} (st value of search space), G_c (list of trajectories in gallery camera), Min (minimum search space), Max (maximize search space)**Output:** g (list of trajectories in gallery)

- 1: **for** $j_g \in G_c$ **do**
 - 2: $d \leftarrow st_j - st_{sch}$
 - 3: **if** $d \geq Min$ **and** $d \leq Max$ **then**
 - 4: $addj_g$ **to** g
 - 5: $g \leftarrow sorted(g)$
 - 6: **return** g
-

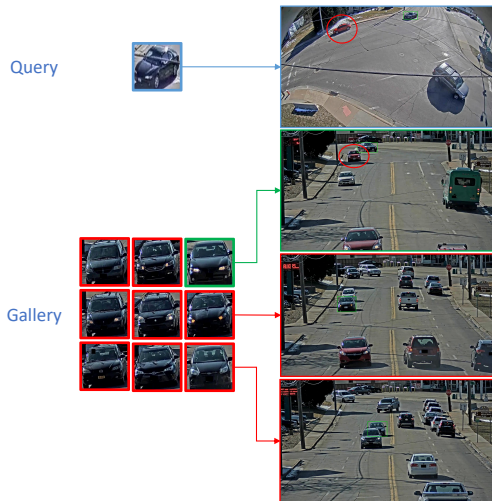


Fig. 6. Employ the background scene from corresponding video clip as side information for cross-camera trajectory matching.

matching errors. A screenshot of the proposed system interface is shown in Fig. 7. Specifically, the lower right part of the interface shows the recommendation list for trajectory matching, the upper right part exhibits the camera location information of the whole area, and the left part displays the video clips of the candidate lists (four candidates' video clips can be displayed simultaneously).

After the cross-camera trajectory matching, the trajectory feature T_i will be structured by,

$$T_i = [(p_i, t_s, t_e, b_i), D_i, f_i], \quad (3)$$

where p_i is the original video data, t_s, t_e are the starting time and the ending time of corresponding video clip, respectively; b_i denotes the bounding box data of T_i ; D_i is the orientation of T_i and f_i is the corresponding feature vector of T_i .

C. System Optimization Regarding Visualization and Adaptability.

The existing re-ID datasets employ a similar visualization methodology that directly marks the trajectory data on the video sequence and stores the visualized trajectory data in video or GIF format. This will cost plenty of storage resources.

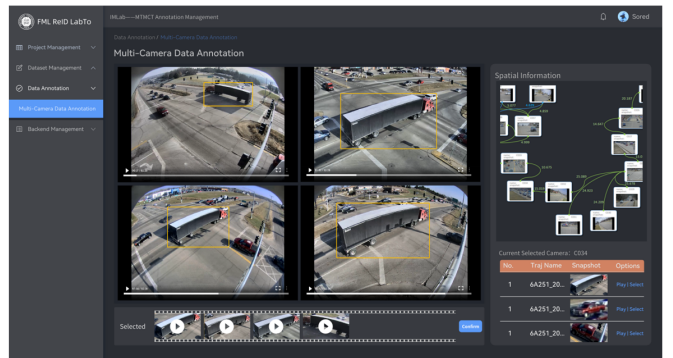


Figure 5. Our Annotation

Fig. 7. **The interface of our system.** The interface provide users visualized camera location information, recommendation list, video clips of recommended candidates.

Instead, the proposed system employs the FFmpeg toolbox to dynamically mark the trajectory data and visualize it via the web. This allows the system to only store the video segments and trajectory features, saving plenty of storage and transfer resources.

We also devote plenty of effort to the system's adaptability and scalability. Specifically, we employ the Linux Container to modularize different sub-tasks and AMQP for different modules' communication. This strategy allows the proposed system to dynamically modularize the sub-tasks according to actual hardware environments, adapting to various application scenarios. An intuitive illustration is shown in Fig. 8. In addition, the proposed system also supports multi-person online collaboration. To achieve this, we employ a parallel processing strategy for the client-end and server-end. The client-end employs the Vue framework to realize the visualization and interaction of the interface, and the server-end realizes dynamic data communication and semi-automatic algorithm inference through flask. Furthermore, to improve the user experience of multi-user online collaboration and avoid blocking caused by simultaneous operating, the system implements asynchronous processing of requests via thread pools and request queue ranking mechanisms.

IV. EXPERIMENTAL RESULTS

In this section, we evaluate the proposed system from the aspect of trajectory generation accuracy, time complexity and annotation performance. Specifically, we will first introduce the evaluation criteria and the implementation details. The experimental results and corresponding analysis will be subsequently presented.

A. Implement Details and Evaluation Criteria

As for the deep-learning-based trajectory generation evaluation, we roughly follow the method employed in [35] [36]. Specifically, the true-positive identities (IDTP, the matching degree of extracted trajectory and ground-truth is more than 80%), false-positive identities (IDFP), and false-negative identities (IDFN, the matching degree of extracted trajectory and

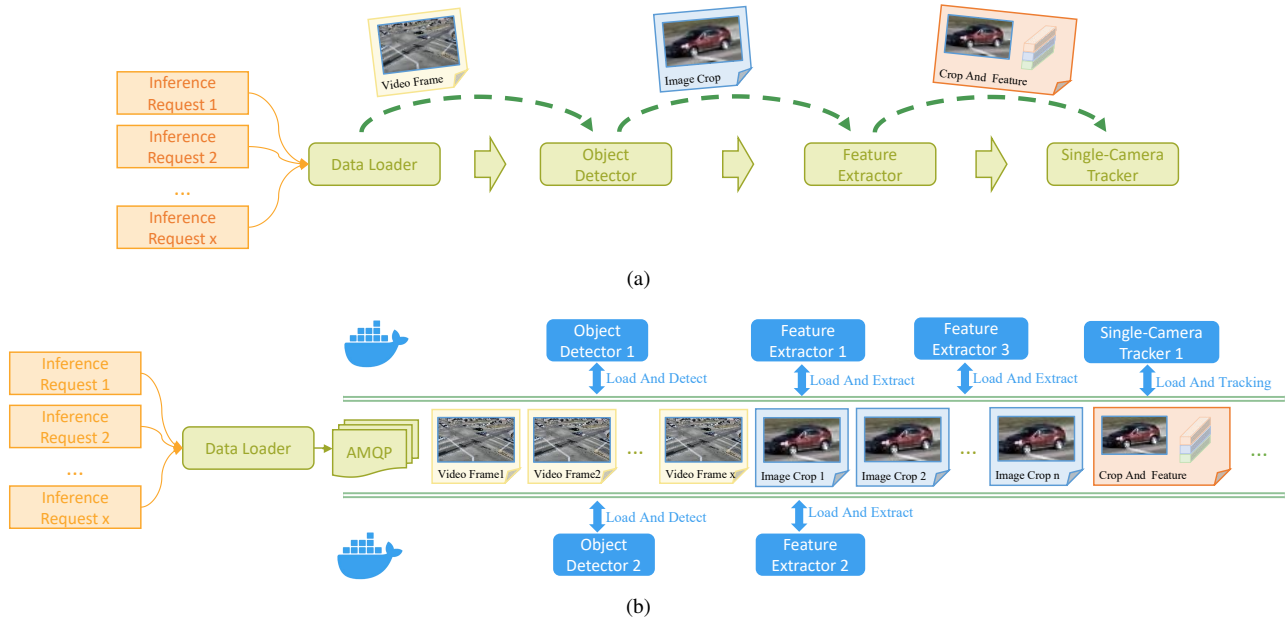


Fig. 8. Comparison between the traditional linear pipeline and the proposed system. (a) Traditional linear pipeline]; (b) Flexible deployment through Linux Container and advanced message queuing protocol (AMQP).

ground-truth is less than 20% or the system fails to generate the trajectory) would be first calculated, and subsequently contributed to the *Precision* and *Recall* computation,

$$Precision = \frac{IDTP}{IDTP + IDFP}, \quad (4)$$

$$Recall = \frac{IDTP}{IDTP + IDFN}. \quad (5)$$

Precision and *Recall* count for the accuracy of deep-learning based trajectory generation. Higher values mean more reliable trajectories generated by the proposed system. The experimental environment is exhibited in table II. As for the object detection module, we employ the YOLOv5x [29] model trained by COCO dataset. The confidence threshold is adjusted to 0.1 to achieve high *Precision* and *Recall* values. In terms of single-camera MOT module, we adjust the time threshold to 1 second and the IoU threshold of the trajectory moving distance to 0.05 to filter the generated trajectories. The proposed system employs a parallel processing strategy of performing these modules on different GPUs to improve generation efficiency. We test the deep-learning-based trajectory generation on the CityFlow [14] dataset, and the initial frame rate is set to 10 frame-per-second. Things have to be mentioned that we discard videos barely containing trajectory data to avoid unnecessary errors in the experimental stage.

B. Experiment Result

1) **Evaluation of Deep-Learning-based Trajectory Generation:** The experimental results are shown in Table III, where 'S#' denotes the scene number in CityFlow [14] and 'c#' is the corresponding camera ID. Quite encouraging

TABLE II
TESTING ENVIRONMENT.

Name	Performance
CPU	Intel Xeon(R) Silver 4210R CPU@2.40GHz×40
GPU	Intel NVIDIA GeForce RTX-3090×2
Memory	256GB
Disk	4TB
System	Ubuntu18.04 LTS






results have been shown, that the proposed deep-learning-based trajectory generation's accuracy reaches 86.98% and 86.81% regarding *precision* and *recall* on average. This provides strong evidence that the proposed system is capable of handling actual application scenarios. Moreover, the system also supports the users in changing the trajectory generation algorithm according to actual needs, which should be owed to the low-coupling modular design.

2) **Evaluation Of the Proposed Trajectory Generation Method's Scalability:** As mentioned in Sec.III, the proposed system provides a scalable setting. Specifically, by adjusting the frame sample interval, users are allowed to have a trade-off between the running time and inferring accuracy. This ensures the proposed system can be adapted to different application scenarios. Here, we conduct extensive experiments with different frame sample intervals to provide guidance for actual applications. And the corresponding running time, *recall* and extraction quality are reported in Table IV and Fig. 9, where the 'Abnormal' refers to situations of failing to generate bounding boxes, extract target vehicles and extract trajectories. As is shown, when the sample interval is higher than 5, the system's performance drops significantly regarding recall rate and the quality of the trajectory generation. By adjusting the

TABLE III
EXPERIMENTAL RESULTS OF DEEP-LEARNING-BASED TRAJECTORY GENERATION.

Name	Algorithm	Ground-Truth	Precision (%)	Recall (%)
S01	c003	79	71	89.87
	c005	80	93	90.00
S02	c006	120	123	93.33
	c009	125	136	92.00
S04	c030	18	23	94.45
	c033	19	26	100.00
	c034	28	24	78.57
	c036	22	21	77.27
S05	c010	45	28	55.56
	c016	84	80	84.52
	c017	76	84	96.05
	c018	55	58	94.55
	c021	72	67	83.33
	c022	84	83	97.62
	c023	54	83	98.15
	c025	69	86	97.10
	c026	86	89	95.35
	c027	77	77	85.71
	c028	88	69	75.00
	c029	119	109	70.59
	c033	225	204	86.67
	c034	192	169	83.85
c035	195	190	94.36	
c036	137	115	73.72	
Average	-	-	86.98	86.81

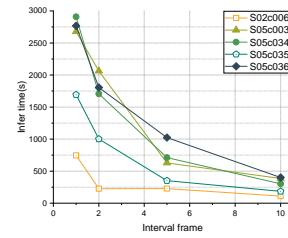
TABLE IV
EXPERIMENTAL RESULTS OF SCALABLE SETTINGS.

Name	Length (s)	FPS	Interval	Infer time (s)	Recall (%)	Observe target	Extract result
S02/c006	211	10	1	746	91.06		Normal
			2	226	60.16		Normal
			5	227	14.63		Abnormal
			10	111	3.25		Abnormal
S05/c033	340	10	1	2,677	95.59		Normal
			2	2,063	84.31		Normal
			5	628	70.10		Normal
			10	386	40.20		Abnormal
S05/c034	342	10	1	2,908	95.27		Normal
			2	1,706	84.52		Normal
			5	711	40.24		Abnormal
			10	303	11.24		Abnormal
S05/c035	347	10	1	1,693	96.84		Normal
			2	1,001	85.26		Normal
			5	351	50.56		Normal
			10	185	11.05		Abnormal
S05/c036	343	10	1	2,768	87.83		Normal
			2	1,805	77.39		Normal
			5	1,024	62.61		Abnormal
			10	400	39.13		Normal

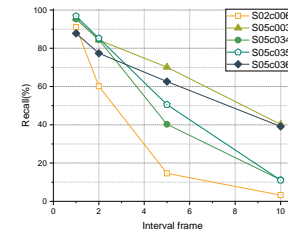
frame sample interval to 2, the system can achieve favorable performance with acceptable time complexity.

3) Verification of Dynamic Annotation Data Loading:

As mentioned in Sec. III, the proposed system employs a novel visualization strategy for annotated trajectory, which greatly reduces the storage requirements. This part compares the storage requirements between the proposed strategy and conventional methods that visualize the trajectories via GIF or video files. The results are shown in table V and Fig. 10. As is shown, the proposed strategy reduces around 99% of storage requirement compared with the conventional method. In addition, the proposed strategy can provide much better perceptual qualities than the method employing GIF format.



(a)



(b)

Fig. 9. The influence of different parameters of frame extraction on the inference result. (a) Inference Time (s); (b) Recall (%). It can be seen from the line graphs (a) and (b) that as the parameter of frame extraction continues to increase, its running time and recall rate are constantly decreasing.

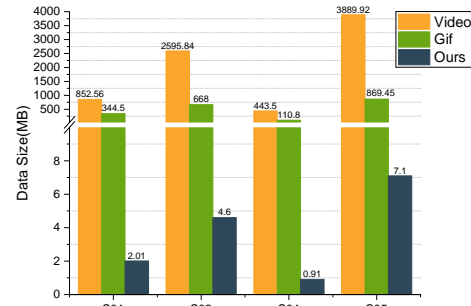


Fig. 10. Illustration of the storage resource requirement among different strategies.

V. CONCLUSION

In this paper, we propose an efficient, accurate, and low-cost semi-automatic MTMCT data annotation system. The system first employs state-of-the-art learning-based object detection, re-ID and MOT algorithms to automatically generate single-camera trajectory features. In the following manual cross-camera trajectory matching process, the system makes full use of side information including timestamp, camera location and background scene to provide users a reliable recommendation list. This would significantly improve the matching accuracy and efficiency. In addition, plenty of efforts have been devoted to system optimization. To be specific, the dynamic annotation data loading saves quite a storage requirement comparing with the conventional annotation data visualization method. And the

TABLE V
EVALUATION OF DYNAMIC ANNOTATION DATA LOADING STRATEGY

	Name	Length (s)	Original video size (MB)	Trajectory visual size (MB)		Ours (MB)
				Video	Gif	
S01	c003	199	151	1,157	376	2.94
	c005	211	55	548	313	1.08
S02	c006	211	292	2,468	587	5.09
	c009	211	205	2,724	749	4.10
S04	c030	63	45	202	68	0.96
	c033	35	43	368	97	0.76
	c034	41	53	605	156	0.83
	c036	36	55	599	122	1.08
S05	c010	407	473	1,761	401	2.45
	c016	394	425	1,843	533	3.93
	c017	387	552	1,823	374	6.37
	c018	384	593	2,836	728	15.20
	c021	400	435	1,331	387	4.55
	c022	427	611	2,560	544	6.00
	c023	425	1,004	3,533	893	9.21
	c025	428	546	1,731	668	10.40
	c026	417	675	4,567	983	3.69
	c027	384	600	4,506	936	3.46
	c028	382	434	4,291	1,055	8.89
	c029	354	768	6,871	1,085	6.75
	c033	340	553	8,602	1,751	9.22
	c034	342	679	7,987	1,444	6.28
	c035	347	346	3,164	931	8.77
	c036	343	429	4,833	1,198	8.50
Average	-	-	-	2,954.58	682.46	5.44

implemented flexible deployment strategy allows multi-person online collaboration. The proposed system considerably contributes to MTMCT studies, allowing researchers to establish large-scale datasets with acceptable human labor and time cost.

ACKNOWLEDGMENT

This work was supported in part by the National Natural Science Foundation of China (Grant 61871270), in part by the Shenzhen Natural Science Foundation under Grants JCYJ20200109110410133 and 20200812110350001.

REFERENCES

- [1] W. Liu, O. Camps, and M. Sznajder, "Multi-camera multi-object tracking," *arXiv preprint arXiv:1709.07065*, 2017.
- [2] C. Liu, Y. Zhang, H. Luo, J. Tang, W. Chen, X. Xu, F. Wang, H. Li, and Y.-D. Shen, "City-scale multi-camera vehicle tracking guided by crossroad zones," in *Proceedings of the IEEE/CVF Conference on Computer Vision and Pattern Recognition*, pp. 4129–4137, 2021.
- [3] J. Ye, X. Yang, S. Kang, Y. He, W. Zhang, L. Huang, M. Jiang, W. Zhang, Y. Shi, M. Xia, *et al.*, "A robust mtmc tracking system for ai-city challenge 2021," in *Proceedings of the IEEE/CVF Conference on Computer Vision and Pattern Recognition*, pp. 4044–4053, 2021.
- [4] M. Wu, Y. Qian, C. Wang, and M. Yang, "A multi-camera vehicle tracking system based on city-scale vehicle re-id and spatial-temporal information," in *Proceedings of the IEEE/CVF Conference on Computer Vision and Pattern Recognition*, pp. 4077–4086, 2021.
- [5] M. Naphade, S. Wang, D. C. Anastasiu, Z. Tang, M.-C. Chang, X. Yang, Y. Yao, L. Zheng, P. Chakraborty, C. E. Lopez, *et al.*, "The 5th AI City Challenge," in *Proceedings of the IEEE/CVF Conference on Computer Vision and Pattern Recognition*, pp. 4263–4273, 2021.
- [6] D. S. Cheng, M. Cristani, M. Stoppa, L. Bazzani, and V. Murino, "Custom pictorial structures for re-identification," in *Bmvc*, vol. 1, p. 6, Citeseer, 2011.
- [7] N. Martinel and C. Micheloni, "Re-identify people in wide area camera network," in *2012 IEEE computer society conference on computer vision and pattern recognition workshops*, pp. 31–36, IEEE, 2012.
- [8] B. Yang, J. Yan, Z. Lei, and S. Z. Li, "Aggregate channel features for multi-view face detection," in *IEEE international joint conference on biometrics*, pp. 1–8, IEEE, 2014.
- [9] S. Ren, K. He, R. Girshick, and J. Sun, "Faster r-cnn: Towards real-time object detection with region proposal networks," *Advances in neural information processing systems*, vol. 28, 2015.

- [10] L. Zheng, Z. Bie, Y. Sun, J. Wang, C. Su, S. Wang, and Q. Tian, "Mars: A video benchmark for large-scale person re-identification," in *European conference on computer vision*, pp. 868–884, Springer, 2016.
- [11] L. Wei, S. Zhang, W. Gao, and Q. Tian, "Person transfer gan to bridge domain gap for person re-identification," in *Proceedings of the IEEE conference on computer vision and pattern recognition*, pp. 79–88, 2018.
- [12] M. Ye, J. Shen, G. Lin, T. Xiang, L. Shao, and S. C. Hoi, "Deep learning for person re-identification: A survey and outlook," *IEEE Transactions on Pattern Analysis and Machine Intelligence*, 2021.
- [13] T. Zhao, S. Liao, and Z. Lei, "Semi-automatic data annotation tool for person re-identification across multi cameras," in *2018 IEEE International Conference on Big Data (Big Data)*, pp. 4672–4677, IEEE, 2018.
- [14] Z. Tang, M. Naphade, M.-Y. Liu, X. Yang, S. Birchfield, S. Wang, R. Kumar, D. Anastasiu, and J.-N. Hwang, "Cityflow: A city-scale benchmark for multi-target multi-camera vehicle tracking and re-identification," in *Proceedings of the IEEE/CVF Conference on Computer Vision and Pattern Recognition*, pp. 8797–8806, 2019.
- [15] D. Gray and H. Tao, "Viewpoint invariant pedestrian recognition with an ensemble of localized features," in *European conference on computer vision*, pp. 262–275, Springer, 2008.
- [16] C. C. Loy, C. Liu, and S. Gong, "Person re-identification by manifold ranking," in *2013 IEEE International Conference on Image Processing*, pp. 3567–3571, IEEE, 2013.
- [17] D. Baltieri, R. Vezzani, and R. Cucchiara, "3dpes: 3d people dataset for surveillance and forensics," in *Proceedings of the 2011 joint ACM workshop on Human gesture and behavior understanding*, pp. 59–64, 2011.
- [18] M. Hirzer, C. Beleznaï, P. M. Roth, and H. Bischof, "Person re-identification by descriptive and discriminative classification," in *Scandinavian conference on image analysis*, pp. 91–102, Springer, 2011.
- [19] W. Li, R. Zhao, and X. Wang, "Human reidentification with transferred metric learning," in *Asian conference on computer vision*, pp. 31–44, Springer, 2012.
- [20] W. Li and X. Wang, "Locally aligned feature transforms across views," in *Proceedings of the IEEE conference on computer vision and pattern recognition*, pp. 3594–3601, 2013.
- [21] W. Li, R. Zhao, T. Xiao, and X. Wang, "Deepreid: Deep filter pairing neural network for person re-identification," in *Proceedings of the IEEE conference on computer vision and pattern recognition*, pp. 152–159, 2014.
- [22] P. F. Felzenszwalb, R. B. Girshick, D. McAllester, and D. Ramanan, "Object detection with discriminatively trained part-based models," *IEEE transactions on pattern analysis and machine intelligence*, vol. 32, no. 9, pp. 1627–1645, 2010.
- [23] L. Zheng, L. Shen, L. Tian, S. Wang, J. Wang, and Q. Tian, "Scalable person re-identification: A benchmark," in *Proceedings of the IEEE international conference on computer vision*, pp. 1116–1124, 2015.
- [24] E. Ristani, F. Solera, R. Zou, R. Cucchiara, and C. Tomasi, "Performance measures and a data set for multi-target, multi-camera tracking," in *European conference on computer vision*, pp. 17–35, Springer, 2016.
- [25] X. Liu, W. Liu, T. Mei, and H. Ma, "A deep learning-based approach to progressive vehicle re-identification for urban surveillance," in *European conference on computer vision*, pp. 869–884, Springer, 2016.
- [26] H. Liu, Y. Tian, Y. Yang, L. Pang, and T. Huang, "Deep relative distance learning: Tell the difference between similar vehicles," in *Proceedings of the IEEE conference on computer vision and pattern recognition*, pp. 2167–2175, 2016.
- [27] P. Wang, B. Jiao, L. Yang, Y. Yang, S. Zhang, W. Wei, and Y. Zhang, "Vehicle re-identification in aerial imagery: Dataset and approach," in *Proceedings of the IEEE/CVF International Conference on Computer Vision*, pp. 460–469, 2019.
- [28] Y. Lou, Y. Bai, J. Liu, S. Wang, and L. Duan, "Veri-wild: A large dataset and a new method for vehicle re-identification in the wild," in *Proceedings of the IEEE/CVF conference on computer vision and pattern recognition*, pp. 3235–3243, 2019.
- [29] J. Redmon, S. Divvala, R. Girshick, and A. Farhadi, "You only look once: Unified, real-time object detection," in *Proceedings of the IEEE conference on computer vision and pattern recognition*, pp. 779–788, 2016.
- [30] Z. Liu, J. Wang, S. Gong, H. Lu, and D. Tao, "Deep reinforcement active learning for human-in-the-loop person re-identification," in *Proceedings of the IEEE/CVF International Conference on Computer Vision*, pp. 6122–6131, 2019.

- [31] J. Zhang, N. Wang, and L. Zhang, "Multi-shot pedestrian re-identification via sequential decision making," in *Proceedings of the IEEE conference on computer vision and pattern recognition*, pp. 6781–6789, 2018.
- [32] Y. Wang, S. Liao, and L. Shao, "Surpassing real-world source training data: Random 3d characters for generalizable person re-identification," in *Proceedings of the 28th ACM international conference on multimedia*, pp. 3422–3430, 2020.
- [33] X. Sun and L. Zheng, "Dissecting person re-identification from the viewpoint of viewpoint," in *Proceedings of the IEEE/CVF Conference on Computer Vision and Pattern Recognition*, pp. 608–617, 2019.
- [34] N. Wojke, A. Bewley, and D. Paulus, "Simple online and realtime tracking with a deep association metric," in *2017 IEEE international conference on image processing (ICIP)*, pp. 3645–3649, IEEE, 2017.
- [35] Y. Zhang, C. Wang, X. Wang, W. Zeng, and W. Liu, "Fairmot: On the fairness of detection and re-identification in multiple object tracking," *International Journal of Computer Vision*, vol. 129, no. 11, pp. 3069–3087, 2021.
- [36] E. Ristani, F. Solera, R. Zou, R. Cucchiara, and C. Tomasi, "Performance measures and a data set for multi-target, multi-camera tracking," in *European conference on computer vision*, pp. 17–35, Springer, 2016.